Journal of Zhejiang University-SCIENCE B (Biomedicine & Biotechnology) in press
www.jzus.zju.edu.cn; www.springer.com/journal/11585
E-mail: jzus_b@zju.edu.cn

Research Article
https://doi.org/10.1631/jzus.B2500239

Protective effect of medium-chain monoglycerides on hepatic lipid accumulation via modulation of bile acid metabolism in Dongliao black pigs

Nanhai XIAO[1], Xutang WANG[2], Jing WANG[1,3], Fengqin FENG[1,4], Minjie ZHAO[1]✉

[1]*College of Biosystems Engineering and Food Science, Zhejiang University, Hangzhou 310058, China*
[2]*Hangzhou Longyu Biotechnology Co., Ltd, Hangzhou 310003, China*
[3]*Ningbo Research Institute, Zhejiang University, Ningbo 315100, China*
[4]*ZhongYuan Institute, Zhejiang University, Zhengzhou 450001, China*

Abstract: The aim of this study was to investigate the effects of feed supplementation with medium-chain monoglycerides (MG) on the growth performance, serum biochemistry, hepatic health, and gut microbiota of Dongliao black pigs. The results showed that 750 mg/kg of MG significantly increased body weight and slaughter rate, while it decreased feed conversion ratio and backfat thickness. In range of 250 mg/kg to 1000 mg/kg MG, there were no significant influences on glucolipid metabolism, the biomarkers of liver and kidney function, and appetite hormones in the serum. However, the control group exhibited massive hepatic lipid deposition, whereas this phenomenon was significantly alleviated after 750 mg/kg of MG intervention. The transcriptome results showed that 750 mg/kg of MG significantly increased the expression of genes related to cholesterol synthesis, cholesterol to bile acid conversion, bile acid glucuronidation, and bile acid reabsorption. Meanwhile, 750 mg/kg of MG prominently enhanced the concentration of total bile acid in the liver and feces. In brief, MG promoted the growth performance and improved the hepatic health of black pigs via the regulation of bile acid metabolism, therefore it has the potential to be used as a feed additive in finishing pigs, with an optimal dietary MG requirement of 750 mg/kg.

Key words: Medium chain monoglyceride; Transcriptome; Bile acid; Cholesterol; Gut microbiota

1 Introduction

Dongliao black pig is a high-quality native pig breed in China, with tender and delicious meat quality—fat but not greasy—which is deeply loved by consumers (Gao et al., 2024). However, compared with foreign pig breeds, Chinese native pigs generally have the disadvantages of slow growth rate, low feed utilization and high breeding costs, making it difficult to gain larger market competitiveness for this breed (Tu et al., 2021). Therefore, developing methods to accelerate the growth rate of native pigs and reduce feed consumption are key to obtaining better market competitiveness. Although animal breeding techniques can obtain pig breeds with stable traits and good meat quality, this approach has many drawbacks such as long-time requirement, complex technology, and huge investment overall. Therefore, there is an urgent need to develop simple and fast techniques. Feed additives are effective ingredients to improve animal production performance, ensure animal health, save feed costs, and improve meat quality (Silveira, Roque-Borda, & Vicente, 2021). This method is easy to apply and is effective, which significantly improves the growth rate of farmed animals and helps farmers achieve higher benefits in a shorter period of time.

Medium-chain monoglycerides (MG) are a group of lipids formed by the esterification of medium chain fatty acids and glycerol, including glycerol monocaprylate (GMC, C8:0), glycerol monodecanoate (GMD, C10:0) and glycerol monolaurate (GML, C12:0) (Liu et al., 2023). Pure medium-chain fatty acids are difficult to

✉ Minjie ZHAO, minjiezhao@zju.edu.cn
Minjie ZHAO, https://orcid.org/0000-0002-5429-9824

Received May 10, 2025; Revision accepted Sept. 25, 2025;
Crosschecked xxx. xx, 20xx; Published online xxx. xx, 20xx

accept by farmed poultry due to their unpleasant odor. By contrast, MG have better stability and functional activities such as antibacterial and antiviral activities, anti-obesity activity, regulation of gut microbiota, and intestinal immunity (Yang et al., 2024). Meanwhile, MG naturally occur in breast milk and coconut oil, and are widely used food preservatives and antibacterial agents (Liu et al., 2021). Recently, many studies have found that MG exerted good regulatory effects on animal health, feed consumption and meat quality. Our previous studies found that 300 mg/kg of MG increased the fresh muscle yield of broilers and improved meat quality with reduced drip loss (Liu et al., 2021). Moreover, MG supplementation increased amino acid concentration and umami compounds to improve the taste of chicken soup (Liu et al., 2021). Currently, the applications of MG (mainly GML) mainly focus on weaned piglets and sows. In one such example, maternal supplementation with GML inhibited the intestinal inflammatory response of piglets (Zhao et al., 2023), and 1000 mg/kg of GML enhanced immune activity and improved intestinal digestibility in weaned piglets (Li et al., 2022). GML supplementation improved the reproductive performance of sows and the growth performance of piglets during late gestation and lactation (Li et al., 2025). These studies confirmed the possibilities of MG application in animal husbandry, whereas the effect of MG on finishing pigs is still unknown.

The present study investigated the effects of dietary MG supplementation on growth performance, serum biochemistry, hepatic health and gut microbiota in black pigs, helping to develop a strategy for optimizing feed formula and increasing breeding benefits.

2 Materials and methods

2.1 Experimental reagents

MG containing GML and GMD with 95% purity (7:3, m/m) was obtained from Hangzhou Longyu Biotechnology Co., Ltd (Hangzhou, China). Glucose, total triglyceride (TG), total cholesterol (TC), low-density lipoprotein cholesterol (LDL-C), high-density lipoprotein cholesterol (HDL-C), alanine aminotransferase (ALT), aspartate aminotransferase (AST), alkaline phosphatase (AKP), blood urea nitrogen (BUN), creatinine (CRE), and total bile acid (TBA) assay kits were purchased from Nanjing Jiancheng Bioengineering Institute (Nanjing, China). Porcine glucagon-like peptide 1 (GLP-1), porcine peptide YY (PYY), porcine neuropeptide Y (NPY), and porcine ghrelin enzyme-linked immunosorbent assay (ELISA) kits were purchased from Wuhan Jiyinmei Biotechnology Co., Ltd (Wuhan, China). Other chemical reagents were obtained from Sinopharm Chemical Reagent Co., Ltd (Shanghai, China), including ethanol, chloroform, methanol, potassium hydroxide, n-hexane, and sodium sulfate.

2.2 Animal experiment

All experimental procedures were approved by the Institutional Animal Ethics Committee of Zhejiang University (ZJU20240866). The experiment was conducted at the premises of Shaoxing Tiansheng Farming Co., Ltd. (Zhejiang, China). A total of 225 black pigs (78 kg of initial weight, sex randomization) were weighed and randomly assigned into five groups (3 replicates/group, 15 pigs/replicate). The farming environment included a controlled condition of 12 h light/12 h dark cycle. The pigs were fed twice every day and were allowed to eat and drink ad libitum. The MG was added into the feed. The composition and nutrient levels of basal diets were shown in the Supplementary Material (Table 1).

The pigs were divided into the following groups:

Control group (NCD): basal diet with no MG

MG250 group (MG250): basal diet with 250 mg/kg of MG

MG500 group (MG500): basal diet with 500 mg/kg of MG

MG750 group (MG750): basal diet with 750 mg/kg of MG

MG1000 group (MG1000): basal diet with 1000 mg/kg of MG

After 3 days of adaptive cultivation, the official experimental period was 50 days, making the whole experiment last for 53 days. During this period, the health status of the pigs was observed; any sick pigs were immediately removed and their weights were recorded. At the end of the feeding trial, the black pigs were fasted

overnight and then butchered on the next day after weight measurement. Blood samples were collected from porcine precaval veins. The supernatant of blood samples was obtained by centrifugation at 3000 g/min for 15 min at 4℃. Liver and fresh rectal feces were collected, and samples were stored at -80 ℃. Meanwhile, the carcass weight and thickness of backfat were measured.

2.3 Growth performance

Growth performance indicators included initial weight ($BW_{initial}$), final weight (BW_{final}), net weight gain (BW_{net}), average daily weight gain (ADG), average daily feed intake (ADFI), feed conversion ratio (FCR), slaughter rate (SR), and backfat thickness (BT). The specific calculation formulas were as follows:

BW_{net} (kg/replicate) = final weight – initial weight

ADG (g/day) = net weight gain / experimental days * 1000

ADFI (kg/day/pig) = total feed eaten / experimental days / the number of pigs per replicate

FCR = total feed eaten / total weight gain

BT was defined as the height of the fat at the back between the sixth and seventh ribs in the front row.

SR was defined as the ratio of carcass weight to fresh weight (excluding the head, hooves, tail, hair, blood, and internal organs).

2.4 Biochemical assays

The concentrations of glucose, TC, TG, LDL-C, HDL-C, ALT, AST, AKP, BUN and CRE were determined using commercial reagent kits from Nanjing Jiancheng Bioengineering Institute (Nanjing, China). The concentrations of GLP-1, PYY, NPY, and ghrelin were measured using ELISA kits according to the manufacturer's protocols.

2.5 Histological analysis

Fresh liver tissue was fixed using a 4% paraformaldehyde solution. Hematoxylin and eosin (H&E) staining and oil red O staining were performed using the standard method, followed by observation of the stained tissues under a microscope. The analysis and calculation were performed using Image J software.

2.6 Liver lipid content

A total of 0.1 g of liver tissue was weighted, and 1 mL of non-water ethanol was added for tissue homogenization. Then, the homogenized solution was treated on a constant temperature shaker for 6 h. After centrifugation at 13,000×g for 15 min at 4℃, the supernatant was obtained, and the concentrations of TC, TG, LDL-C, and HDL-C in the liver were analyzed using commercial reagent kits. The extraction steps of total liver lipids were similar to the above steps. The extraction solvent was changed to chloroform - methanol (2:1, v/v). Total liver lipids were collected and weighted after performing the solvent evaporation method.

2.7 Fatty acid composition

The extraction steps of total liver lipids were similar to the above steps. Next, 0.04 g of lipid sample was dissolved in 2 mL of n-hexane, and 0.2 mL of methanol-potassium hydroxide solution (2 mol/L) was added. After homogeneous mixing, 1 g of sodium sulfate was added to obtain the upper organic phase. Then, the organic phase was collected and filtered for gas chromatography analysis. The specific instrument parameters were the same as in our previous work (Liu et al., 2023).

2.8 Transcriptome

Total RNA was extracted from fresh liver tissue using the commercial RNA extraction kit (Yiside, Hangzhou, China). Nanodrop2000 (Thermo Fisher Scientific, USA) was used to detect the concentration and purity of the extracted RNA, and agarose gel electrophoresis was used to detect the integrity of RNA. After enriching and reverse transcription, RNA sequencing was performed using the Novaseq 6000 platform (Illumina, USA). Following quality evaluation and filtration, a total of 69.3 Gb of clean data was obtained, in which each sample had clean data of 6.1 Gb or more, and the Q30 base percentage was over 95.82%. By aligning the clean data of each sample with the reference genome, the alignment rates ranged from 96.53% to 97.14%. Based on the quantitative results, differential gene analysis between the two groups was performed using DESeq2 software and the screening threshold was $|\log_2$ fold change $|>=1$ and p value < 0.05. Functional enrichment analysis based on the KEGG database was performed according to the principle of p adjust < 1. The

reference gene source was Sus_Scrofa and the reference genome version was sscrofta11.1. The reference genome source can be found at http://asia.ensembl.org/Sus_scrofa/Info/Index.

2.9 Gene expression

A total of 10-20 mg of liver tissue was weighted and placed in a 2 mL centrifuge tube, then added with 1 mL of trizol lysis buffer in each tube. Then, a commercial RNA extraction kit was used to extract total RNA. The concentration and purity of RNA products were measured using a Nanodrop spectrophotometer. Then, cDNA synthesis was performed using the HiScript III RT SuperMix reverse transcription kit (Vazyme, Nanjing, China). Finally, a real-time fluorescence quantitative PCR reaction was conducted using the ChamQ SYBR Color qPCR Master Mix fluorescence quantitative reagent kit (Vazyme, Nanjing, China). The primer design was sourced from the NCBI database. The relative expression levels of each gene were calculated using the $2^{-\Delta\Delta t}$ method with GAPDH as the internal reference. The primer sequences were shown in Supplementary Material (Table 2).

2.10 Gut microbiota analysis

Genomic DNA was extracted from the rectal feces according to the commercial kit instructions, and the quality of the extracted DNA was detected by agarose gel electrophoresis. PCR amplification was performed and the universal primer sequences were 338F (ACTCCTACGGGAGGCAGCAG) and 806R (GGACTACHVGGGTWTCTAAT). The PCR products were amplified using the QuantiFluor™-ST blue fluorescence quantification system (Promega, China), and sequencing was performed using the Illumina Hiseq2500 PE 250 instrument. After quality control and the filtration of raw reads, FLASH software (1.2.11) was used to obtain optimized data. Then, the sequence denoising method (DADA2) was utilized to process the optimized data, and sequences with a similarity greater than 97% were classified as Operational Taxonomic Units (OTU). On the basis of OTU representative sequences and abundance information, a series of statistical or visual analyses were conducted, such as abundance-based coverage estimator (ACE) index, Principal coordinate analysis (PCoA), species difference analysis, and correlation analysis, with the following specifics: Species annotation database: silva138/16s_bacteria, species annotation method: classify sklarn (Naive Bayes), classification confidence: 0.7, sequence denoising method: DADA2, quality control: fastp (v0.19.6), splicing: FLASH (v1.2.7).

2.11 Determination of total bile acid concentrations and fecal lipid content

A total of 0.1 g of fecal sample was ground after adding 1 mL of methanol, and placed on a constant temperature shaker for 6 h. Then, the supernatant was extracted after centrifugation at 13,000×g for 15 min at 4℃. The TG and TC contents were determined using commercially reagent kits. The extraction of total lipids in feces was similar to the above steps, but the extraction solvent was changed to chloroform-methanol (2:1). Total lipid was obtained after removing the organic solvent by a nitrogen blower. Then, the total lipid was weighed and the fat yield was calculated. The concentrations of total bile acids in different tissues were measured using commercial reagent kits.

2.12 Statistical analysis

The results were presented as mean ± standard error of the mean (SEM). Statistical analysis was performed using SPSS Statistics 26 software (IBM Analytics, USA). Comparisons between groups were analyzed using one-way analysis of variance (ANOVA) and Student's t test, followed by multiple comparisons by the Dunnett test or Tamhane's test. $p < 0.05$ was considered statistically significant.

3 Results

3.1 MG enhanced the growth performance of pigs

In order to visually evaluate the effect of MG on the growth of black pigs, the growth and slaughter performances were analyzed. As shown in Table 1, during the entire experimental period, the BW_{net}, ADG, ADFI, and FCR of the NCD group were 25.54 kg, 464.52 g/d, 2.78 kg/d, and 5.04, respectively. In the dosage range of 250-1000 mg/kg of MG, there were no dose-dependent relationships between the NCD group and other groups on the BW_{final}, BW_{net}, ADG, ADFI, and FCR. Among them, the BW_{final} of the MG250 group and MG750

group were significantly higher than the NCD group, and both groups showed similar trends in BW_{net}, ADG, ADFI, and FCR. However, poorer growth-promoting effects were observed in the MG500 and MG1000 groups. Overall, MG at 250 mg/kg and 750 mg/kg dosages promoted weight gain in black pigs. Compared with the NCD group, the cold carcass weight of the MG250 group decreased by 1.27%, while that of the MG500, MG750 and MG1000 groups increased by 0.66%, 1.69% and 0.57%, respectively, indicating that 250 mg/kg of MG resulted in lower pork yields. Although 250 mg/kg of MG could promote weight gain, this may have been related to blood and visceral weight, and not to the contribution of meat weight. Backfat thickness reflected the degree of subcutaneous fat deposition and was directly related to lean meat percentage. Generally, a larger backfat thickness indicates that pigs are more obese and have a lower lean meat percentage. Table 1 shows that low (250 mg/kg) or high (1000 mg/kg) doses of MG increased backfat thickness in black pigs, indicating that these doses caused a massive deposition of subcutaneous fat, while 500 mg/kg and 750 mg/kg of MG obviously reduced backfat thickness. Overall, the MG500 and MG750 groups exhibited the best slaughter performance.

Table 1 Effect of MG with different concentration on growth performance

Growth performance	CON	MG250	MG500	MG750	MG1000
$BW_{initial}$ (kg)	78.56±1.62	78.42±1.24	78.33±0.22	78.44±2.04	78.55±1.29
BW_{final} (kg)	104.10±1.24^{c}	107.49±1.07^{a}	104.94±0.12^{bc}	107.11±0.91^{ab}	105.12±0.95^{bc}
BW_{net} (kg)	25.54±2.86	29.07±2.32	26.61±0.10	28.67±2.39	26.57±0.49
ADG (g/d)	464.52±52.82	532.90±54.52	487.06±11.61	527.79±44.54	492.26±15.66
ADFI (kg/d)	2.78±0.04	2.82±0.13	2.77±0.06	2.89±0.11	2.76±0.05
FCR	5.04±0.36	4.59±0.31	5.02±0.09	4.72±0.13	4.83±0.14
SR (%)	72.06±1.39^{ab}	70.79±2.22^{b}	72.72±1.20^{a}	73.75±1.66^{a}	72.63±2.23^{a}
BT (cm)	3.71±0.56^{ab}	4.05±0.32^{a}	3.28±0.38^{b}	3.58±0.56^{ab}	4.08±0.73^{a}

$BW_{initial}$: initial weight, BW_{final}: final weight, BW_{net}: net weight gain, ADG: average daily weight gain, ADFI: average daily feed intake, FCR: feed conversion ratio, SR: slaughter rate, BT: backfat thickness. In the same row, different letter meant significant difference ($p < 0.05$).

3.2 MG had no significant effect on the serum biochemical indexes

The growth performance results indicated that MG addition caused weight gain and changes in backfat thickness. To exclude the interference of obesity, lipid levels in the serum were measured. As shown in Figures 1a-f, compared with the NCD group, none of the treatment doses of MG (250-1000 mg/kg) had a significant effect on blood glucose, TC, TG, LDL-C, HDL-C, and LDL-C/HDL-C ratio, indicating that MG supplementation maintained the normal serum glucolipid metabolism. To investigate the effect of MG on organ damage, the levels of liver and kidney function biomarkers in the serum were measured. AST, ALT and AKP were considered to characterize liver function, while CRE and BUN were deemed to characterize kidney function. As shown in Figures 1g-k, compared with the NCD group, none of the experimental dosages of MG had a significant effect on the concentration of CRE, BUN, AKP, AST and ALT, indicating that MG in the dosage range of 250-1000 mg/kg was safe for black pigs. To further reveal the reason for the promotive effect of weight gain, appetite hormones in the serum were analyzed. GLP-1 and PYY belong to appetite suppressing hormones, while NPY and ghrelin belong to appetite promoting hormones. As shown in Figures 1l-o, MG at different doses had no significant effect on the levels of GLP-1, PYY, NPY, and ghrelin, indicating that the weight gain of black pigs after MG addition was not attributed to the regulation and secretion of appetite hormones.

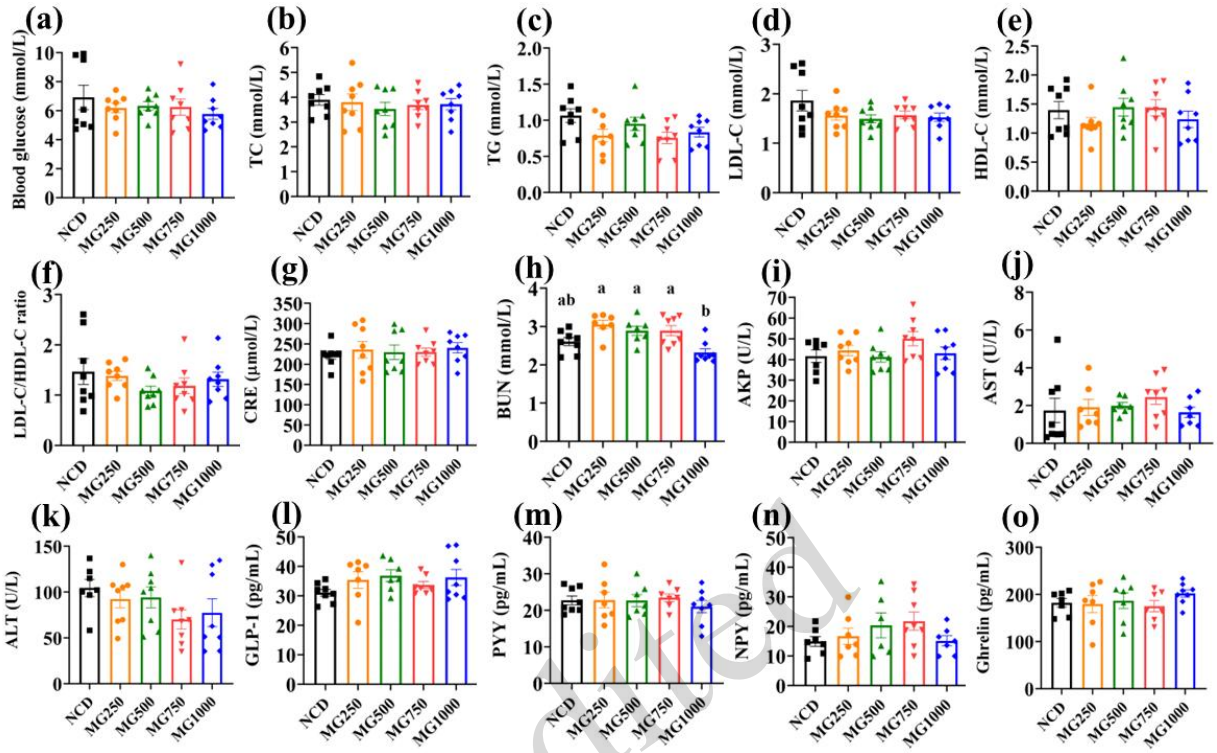

Figure 1 Effect of MG at different doses on serum indexes. (a) Serum blood glucose; (b) serum TC level; (c) serum TG level; (d) serum LDL-C level; (e) serum HDL-C level; (f) LDL-C/HDL-C ratio; (g) CRE level; (h) BUN level; (i) AKP level; (j); AST level; (k) ALT level; (l) GLP-1 level; (m) PYY level; (n) NPY level; (o); ghrelin level. Different letters indicate significant difference ($p < 0.05$). TG: total triglyceride, TC: total cholesterol, LDL-C: low-density lipoprotein cholesterol, HDL-C: high-density lipoprotein cholesterol, CRE: creatinine, BUN: blood urea nitrogen, AKP: alkaline phosphatase, AST: aspartate aminotransferase, ALT: alanine aminotransferase, GLP-1: Porcine glucagon-like peptide 1, PYY: porcine peptide YY, NPY: porcine neuropeptide Y. The values are expressed as mean ± standard error of the mean (SEM), n=6-8.

3.3 MG750 significantly reduced hepatic lipid deposition

To further reveal the impact of MG on the liver health of black pigs, the tissue morphology and lipid content of the liver were analyzed. As shown in Figure 2a, the HE staining result showed that the NCD group had disordered hepatic tissue structure, wrinkled cell morphology, a large number of lipid droplets, and inflammatory cell infiltration. Compared with the NCD group, the MG750 group had intact hepatic tissue structure, full cell morphology, significantly reduced lipid droplets, and no inflammatory cell infiltration. However, other dosages of MG yielded different degrees of lipid droplet accumulation. To evaluate the lipid accumulation in the liver, oil red O staining was used. The results showed that the red proportion of the NCD group was obvious, indicating that the liver of the NCD group exhibited massive lipid deposition (Figure 2b). As the MG dosage increased, the degree of hepatic lipid deposition decreased at first and then increased. A dose of 500 mg/kg MG had the potential to reduce hepatic lipid deposition, but there was no significant difference compared with the NCD group. However, 750 mg/kg of MG significantly reduced hepatic lipid deposition, which could be confirmed from Figure 2c. To further investigate the reason for the decrease in hepatic lipid deposition, the concentrations of TC, TG, HDL-C and LDL-C in the liver were analyzed. As shown in Figures 2d-g, compared with the NCD group, the levels of TG, TC, LDL-C in the MG750 group decreased by 12.66%, 6.055% and 1.14%, respectively, which might be the reason for the decreased hepatic fat in the MG750 group. However, this effect was not dose-dependent because 250 mg/kg and 1000 mg/kg of MG exacerbated hepatic lipid deposition, consistent with the results of backfat thickness. In summary, 750 mg/kg of MG had the best

effect and was therefore selected for mechanism analysis.

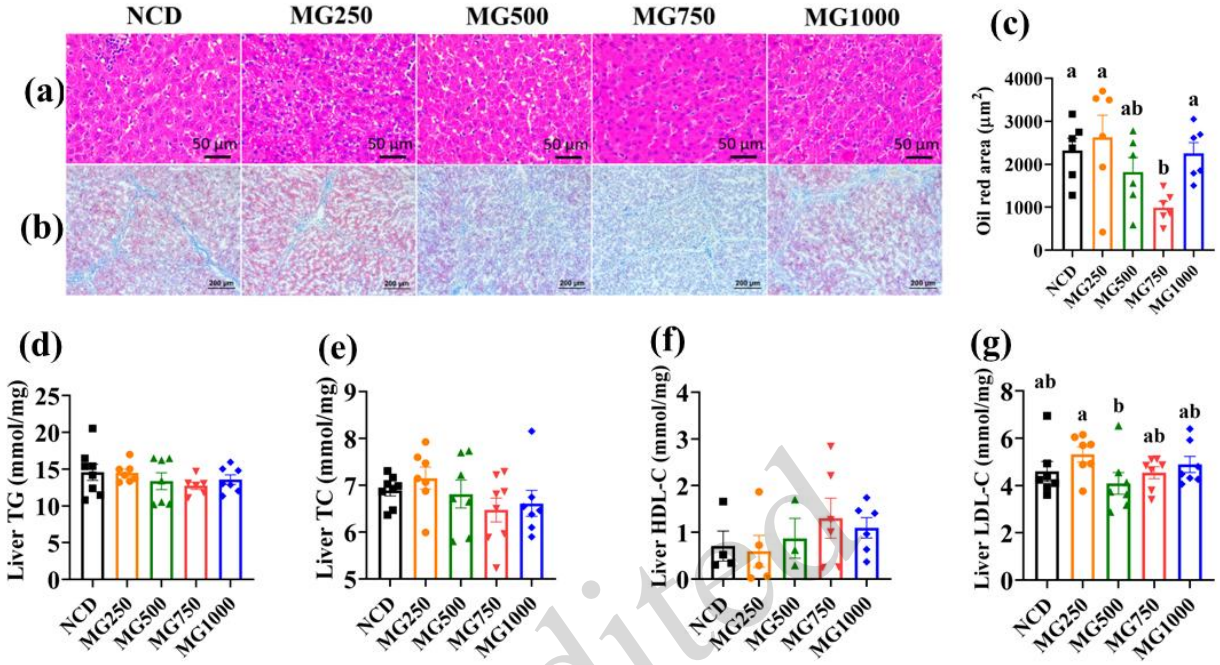

Figure 2 Effect of different doses of MG on hepatic histopathology and lipid content. (a) Representative figure of H&E staining (50 μm); (b) representative figure of oil red O staining (200 μm); (c) result of oil red area; (d) liver TG level; (e) liver TC level; (f) liver HDL-C level; (g) liver LDL-C level. Different letters indicate significant difference ($p < 0.05$). TG: total triglyceride, TC: total cholesterol, LDL-C: low-density lipoprotein cholesterol, HDL-C: high-density lipoprotein cholesterol. The values are expressed as mean ± standard error of the mean (SEM), n=3-8.

3.4 MG had no significant influence on hepatic fatty acid composition

To further investigate the effect of MG on hepatic lipid metabolism, the fatty acid composition of the liver was analyzed. As shown in Table 2, a total of 17 kinds of fatty acids were detected, with the highest levels being those of palmitic acid (C16:0), stearic acid (C18:0), oleic acid (C18:1n9c), linoleic acid (C18:2n6c), and arachidonic acid (C20:4n6). Compared with the NCD group, the MG750 group had no significant regulatory effect on each fatty acid type such as saturated fatty acids (SFA) and unsaturated fatty acids (UFA), but it reduced the content of stearic acid ($p = 0.052$) and increased the content of oleic acid.

Table 2 Effect of MG with different concentration on hepatic fatty acid composition

	NCD	MG750	*p* value
C16:0	15.43±1.38	16.21±0.79	0.252
C16:1	0.73±0.12	0.73±0.07	0.996
C17:0	0.49±0.12	0.53±0.11	0.500
C18:0	22.91±1.58	21.24±1.07	0.052
C18:1n9c	15.56±1.26	16.32±1.60	0.378
C18:2n6c	13.39±0.85	13.26±0.97	0.811
C18:3n6	0.21±0.04	0.25±0.06	0.183
C18:3n3	0.41±0.05	0.44±0.15	0.637
C20:0	0.38±0.08	0.41±0.10	0.606

C20:1	0.20±0.04	0.23±0.11	0.541
C20:2	0.54±0.06	0.55±0.10	0.842
C21:0	0.58±0.12	0.66±0.12	0.242
C20:3n6	0.77±0.19	0.59±0.09	0.062
C20:4n6	18.25±1.80	17.91±1.24	0.715
C22:0	0.41±0.07	0.33±0.07	0.08
C24:0	2.00±0.17	1.98±0.15	0.793
C24:1	0.79±0.19	0.75±0.11	0.661
SFA	42.20±0.65	41.36±1.10	0.134
MUFA	17.29±1.28	18.04±1.67	0.400
PUFA	33.02±0.90	32.45±0.83	0.279
UFA	50.31±0.93	50.49±1.78	0.827

SFA: Saturated fatty acid, UFA: unsaturated fatty acid, MUFA: monounsaturated fatty acid, PUFA: polyunsaturated fatty acid.

3.5 MG750 reduced hepatic lipid accumulation

In order to reveal the mechanism by which MG improves hepatic lipid accumulation transcriptome analysis was performed. As shown in Supplementary Material (Table 3 and Table 4), the Q30 of each sample was greater than 95.82% and total alignment rate of each sample was greater than 96.53%, indicating that the sequencing data had high accuracy and could be used for subsequent analysis. Thus, we further analyzed the differentially expressed genes. As shown in Figure 3a, a total of 10,561 differentially expressed genes were shared between the NCD group and the MG750 group, while 451 genes were specifically expressed in the NCD group and 223 genes were specifically expressed in the MG750 group. The volcano plot (Figure 3b) showed that, compared with the NCD group, 313 differentially expressed genes were significantly upregulated and 257 differentially expressed genes were significantly downregulated in the MG750 group. To characterize the differences between each sample, a clustering heatmap was used, in which red represented significant upregulation and blue represented significant downregulation. As shown in Figure 3d, there were a large number of differentially expressed genes between the two groups. The PCA results (Figure 3c) also proved that the two groups had significant differences in gene expression. To further screen the key signaling pathways associated with differentially expressed genes, the KEGG database was used for functional enrichment analysis. As shown in Figure 3e, the top 20 signaling pathways were enriched, mainly including retinol metabolism, steroid hormone biosynthesis, the PPAR signaling pathway, terpenoid backbone biosynthesis, fatty acid degradation, the Fc epsilon RI signaling pathway, the NF-kappa B signaling pathway, arachidonic acid metabolism, the calcium signaling pathway, the AMPK signaling pathway, and natural killer cell-mediated cytotoxicity. Subsequently, we further analyzed the above signaling pathways, and found that the significantly upregulated genes were mainly related to cholesterol synthesis (*SREBP-1c*, *ACC1*, *FAS*, *SCD-1*, *HMGCR*, *HMGCS*, *MVK*) and bile acid metabolism (*CYP* series, *UGTs*, *SULTs*). On this basis, we assumed that MG750 alleviated hepatic lipid deposition by regulating cholesterol synthesis and bile acid metabolism.

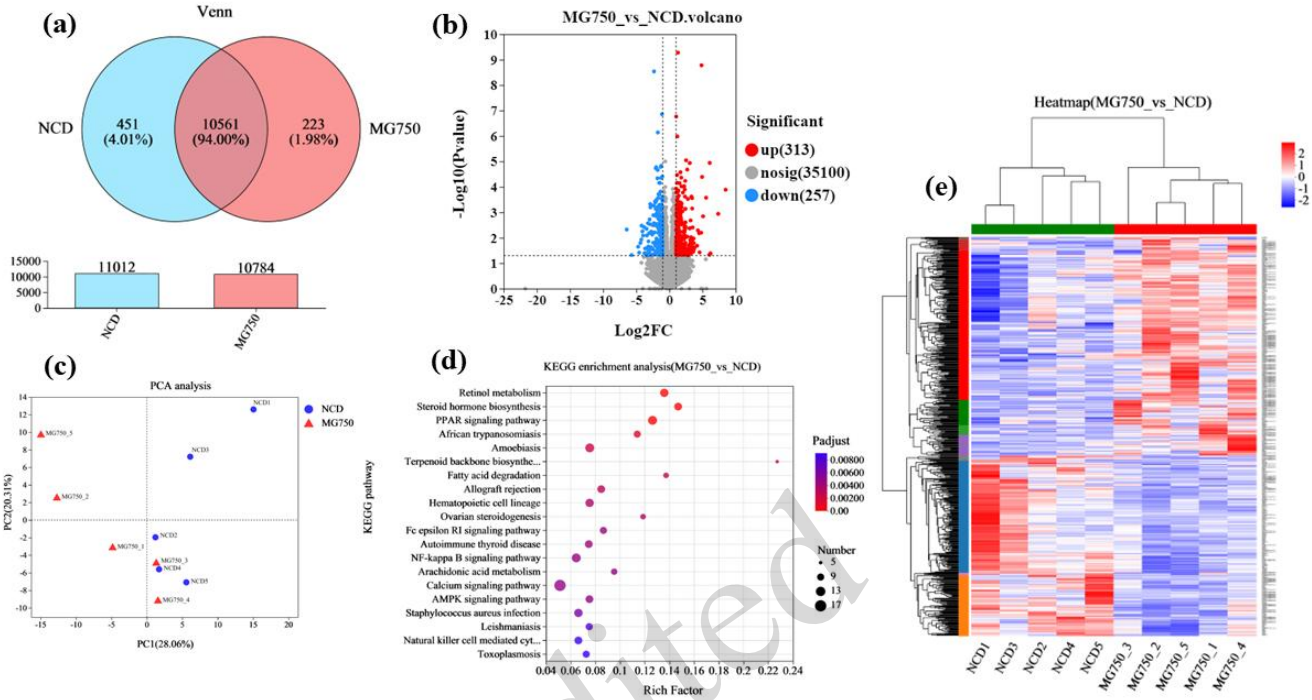

Figure 3 Analysis of hepatic transcriptome. (a) Venn plot of differentially expressed genes; (b) volcano plot of differentially expressed genes (n = 5); (c) principal component analysis (PCA) plot; (d) heatmap of differentially expressed genes; (e) KEGG enrichment analysis.

3.6 MG750 promoted the de novo synthesis of cholesterol

The pathway of cholesterol synthesis was shown in Figure 4a. Compared with the NCD group, MG750 significantly upregulated gene expression related to cholesterol synthesis, including cholesterol acyltransferase 2 (*ACAT2*), HMG-CoA synthase 1 (*HMGCS1*), HMG-CoA reductase (*HMGCR*), mevalonate kinase (*MVK*), phosphomevalonate kinase (*PMVK*), mevalonate diphosphate decarboxylase (*MVD*), farnesyl diphosphate synthase (*FDPS*), farnesyl diphosphate farnesyl transferase 1 (*FDFT1*), squalene epoxidase (*SQLE*), lanosterol synthetase (*LSS*), and 7-dehydrocholesterol reductase (*DHCR7*) (Figure 4b). Therefore, it was suggested that MG750 intervention promoted de novo synthesis of cholesterol. Meanwhile, the gene expressions related to lipid metabolism were also significantly upregulated (Figure 4c), including fatty acid synthetase (*FAS*), sterol regulatory element binding proteins-1c (*SREBP-1c*), Acetyl-CoA carboxylase (*ACC*), Stearoyl-CoA Desaturase 1 (*SCD-1*), carnitine palmitoyltransferase 1 (*CPT-1*). Next, the gene expressions of rate-limiting enzyme were further verified using Q-PCR, and the results showed that MG750 significantly increased the mRNA expression of *HMGCR* (Figure 4d-e), confirming the reliability of the transcriptome results. The gene expressions of *FAS*, *SREBP-1c*, *ACC*, *SCD-1*, *CPT-1* were also upregulated, but there were no significant differences. These results indicated that MG750 promoted the de novo synthesis of cholesterol.

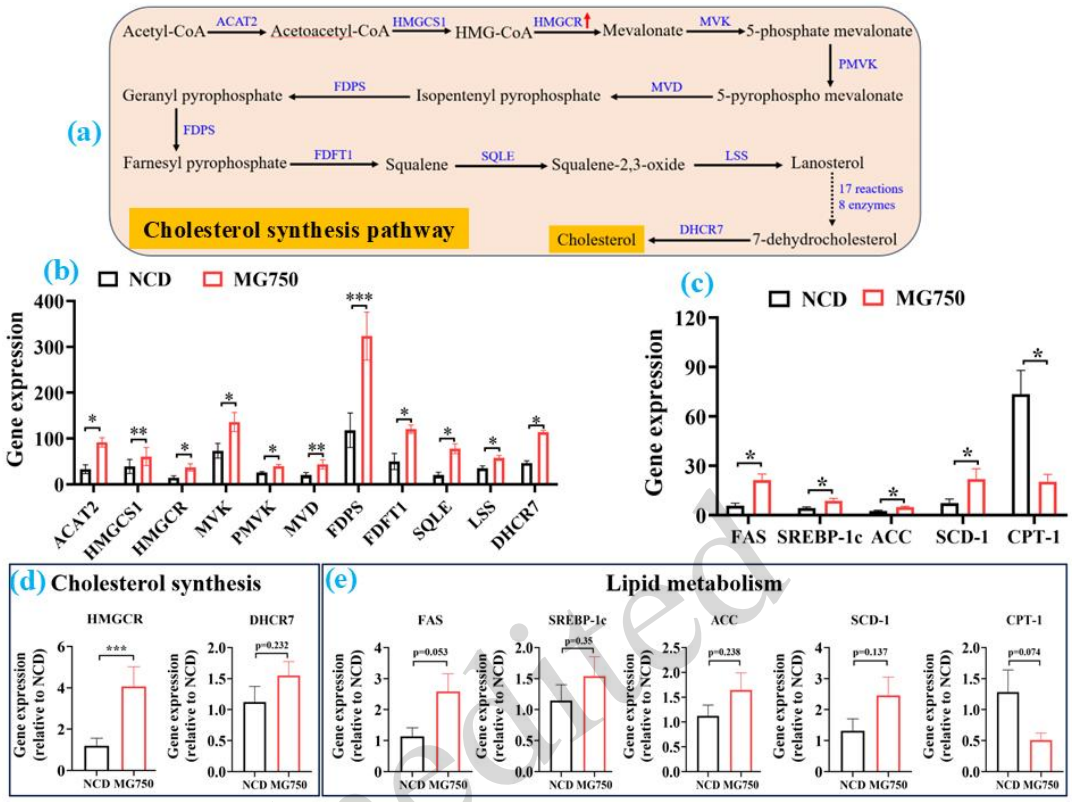

Figure 4 Gene expression related to cholesterol synthesis and lipid metabolism. (a) Pathway of cholesterol synthesis; (b) gene expressions related to cholesterol synthesis; (c) gene expressions related to lipid metabolism; (d) mRNA expressions of rate-limiting enzyme related to cholesterol synthesis; (e) mRNA expressions of key genes related to lipid metabolism. * indicates $p < 0.05$, ** indicates $p < 0.01$, *** indicates $p < 0.001$. *ACAT2*: Cholesterol acyltransferase 2, *HMGCS1*: HMG-CoA synthase 1, *HMGCR*: HMG-CoA reductase, *MVK*: mevalonate kinase, *PMVK*: phosphomevalonate kinase, *MVD*: mevalonate diphosphate decarboxylase, *FDPS*: farnesyl diphosphate synthase, *FDFT1*: farnesyl diphosphate farnesyl transferase 1, *SQLE*: squalene epoxidase, *LSS*: lanosterol synthetase, *DHCR7*: 7-dehydrocholesterol reductase, *FAS*: fatty acid synthetase, *SREBP-1c*: sterol regulatory element binding proteins-1c, *ACC*: Acetyl-CoA carboxylase, *SCD-1*: Stearoyl-CoA Desaturase 1, *CPT-1*: carnitine palmitoyltransferase 1. The values are expressed as mean ± standard error of the mean (SEM), n=5-8. The red arrow represents a significant upregulation.

3.7 MG750 promoted the conversion of cholesterol to bile acids and bile acid metabolism

Figure 5a shows the main pathway of bile acid metabolism. We found that MG750 significantly upregulated the gene expression of cytochrome P450 7A1 (*CYP7A1*) and *CYP27A1*, while *CYP7B1* and *CYP8B1* showed no significant differences (Figure 5b). Then, we analyzed the gene expression related to bile acid excretion. We found that MG750 significantly upregulated the gene expression of UDP-glucuronyl transferase 2B4 (*UGT2B4*), *UGT2A1* and *UGT2C1*, and yielded no significant differences in the gene expression of sulfotransferase 1E1 (*SULT1E1*), *SULT2A1*, *SULT1C4*, *SULT1C2* (Figure 5b), which suggested that MG750 intervention promoted the gluconaldehyde acidification rather than the sulfation of bile acid. Moreover, MG750 significantly up-regulated the gene expression of solute carrier family 10 member 1 (*SLC10A1*), which confirmed that MG750 promoted the reabsorption of bile acid from the blood to the liver. To verify the reliability of the transcriptome results, some key genes were further verified using Q-PCR, including *CYP7A1*, *CYP27A1*, *CYP7B1*, *CYP8B1*, *UGT2B4*, *UGT2C1*, and *SLC10A1*. Compared with the NCD group, 750 mg/kg of MG significantly upregulated the mRNA expression of *CYP7A1*, *UGT2B4* and *SLC10A1* (Figures

5c-d), which was consistent with the trend of transcriptome results. Therefore, MG750 promoted the conversion of cholesterol to bile acids and increased the water solubility and reabsorption process of bile acids, which was helpful to improve enterohepatic circulation and the detoxification process.

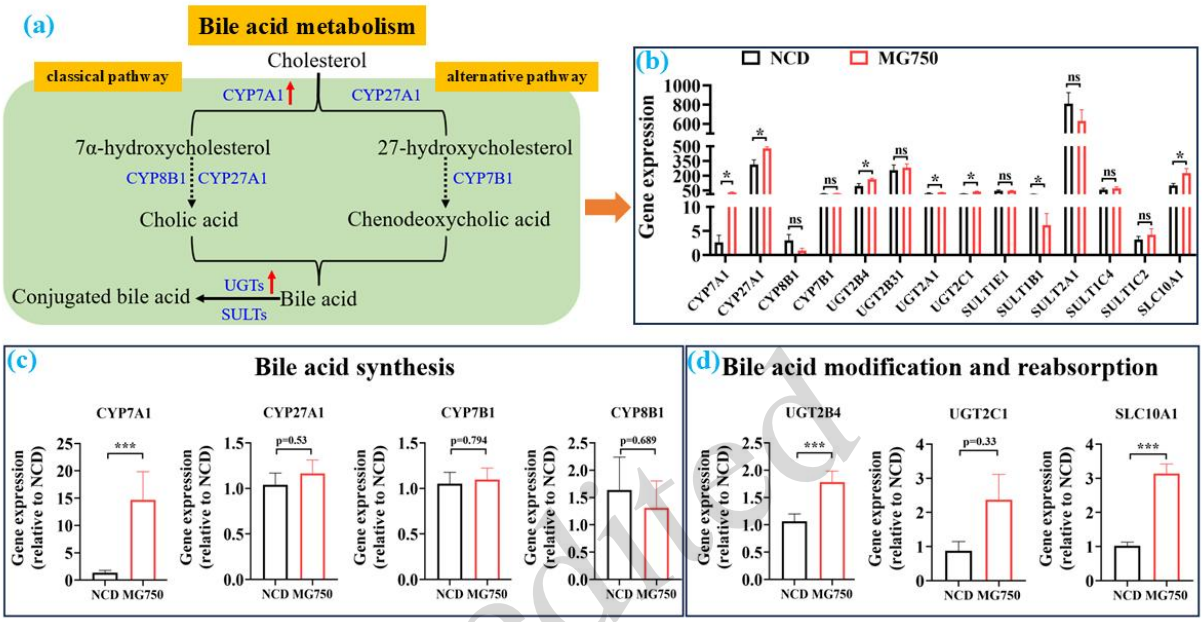

Figure 5 Gene expression related to bile acid metabolism. (a) Pathway of bile acid metabolism; (b) gene expressions related to bile acid metabolism; (c) mRNA expressions of genes related to bile acid synthesis; (d) mRNA expressions of genes related to bile acid modification and reabsorption. * indicates $p < 0.05$, *** indicates $p < 0.001$. *CYP*: cytochrome P450, *UGT*: UDP-glucuronyl transferase, *SULT*: sulfotransferase, *SLC10A1*: solute carrier family 10 member 1. The values are expressed as mean ± standard error of the mean (SEM), n=5-8. The red arrow represents a significant upregulation.

3.8 MG750 increased the concentration of TBA and promoted fecal lipid excretion

The above results confirmed that MG750 significantly promoted the gene expression related to bile acid synthesis and excretion. To verify this conclusion, the total bile acid (TBA) contents in different tissues were measured. As shown in Figures 6a-c, compared with the NCD group, 750 mg/kg of MG significantly increased the TBA content in the liver and feces, indicating that MG promoted the synthesis and excretion of bile acid. In addition, there was no significant difference in TBA content in the serum. We also measured the level of fecal lipids, and found that total lipids, TG and TC content in the feces of the MG750 group increased by 13.7%, 17.67% and 11.91%, respectively (Figure 6d-f), which stated that MG supplementation was beneficial for lipid excretion from feces.

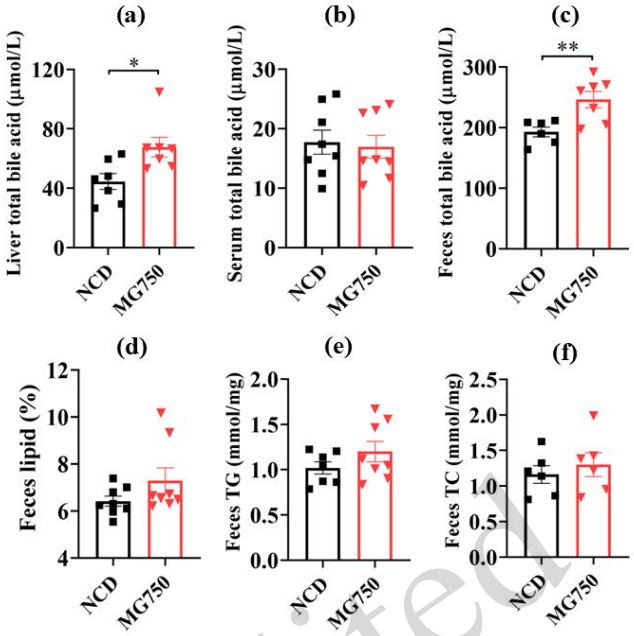

Figure 6 Analysis of total bile acid and fecal lipids. (a) Concentration of total bile acid in the liver; (b) Concentration of total bile acid in the serum; (c) concentration of total bile acid in the feces; (d) content of total lipids in the feces; (e) content of TG in the feces; (f) content of TC in the feces. * indicates $p < 0.05$, ** indicates $p < 0.01$. The values are expressed as mean ± standard error of the mean (SEM), n=6-8. TG: total triglyceride, TC: total cholesterol.

3.9 Effect of different doses of MG on gut microbiota

The gut microbiota is closely related to the growth performance and health status of pigs. To explore the impact of MG at different doses on gut microbiota, we analyzed the abundance changes of gut microbiota. As shown in Figure 7a-f, the five groups had 182 of shared OTUs, and the special OTUs of the NCD group, MG250 group, MG500 group, MG750 group, and MG1000 group were 23, 10, 12, 24, and 13, respectively. Alpha diversity includes the ACE index, Chao index, Shannon index, and Simpson index, which reflect the diversity and richness of gut microbiota. There were no significant differences in ACE index, Chao index, Shannon index, and Simpson index among the five groups (except for a significant difference in Chao index between the MG750 group and the MG250 and MG500 groups), indicating that the addition of MG had no significant effect on the relative abundance and diversity of gut microbiota. The PCoA result also mirrored these findings.

At the phylum level (Figure 7g), compared with the NCD group, the Firmicutes / Bacteroidetes ratios were significantly increased with increasing MG dose, and the abundance of Bacteroidetes was significantly decreased at 1000 mg/kg of MG. Especially, the relative abundance of Proteobacteria at 1000 mg/kg of MG was significantly increased, whereas the abundances of the other four groups were relatively lower. Figure 7h shows the relative abundance of the top 10 differential bacteria at the genus level, mainly including *Lachnospiraceae*, *Ruminococcus*, *Rikenellaceae*, *Holdemanella*, *Ruminococcaceae*. Compared with the MG250 and MG500 groups, MG750 significantly decreased the relative abundance of *Lachnospiraceae* and *Ruminococcus* (figure 7i-j), while there was no significant difference between the MG750 and NCD groups. The results showed that the relative abundance of *Escherichia/Shigella* (a genus of Proteobacteria) in the MG1000 group was significantly higher than that in the NCD group. Spearman's correlation analysis revealed that the increase in the abundance of *Escherichia/Shigella* and *Ruminococcus* was negatively correlated with weight gain and ADG and positively correlated with hepatic TC and TG.

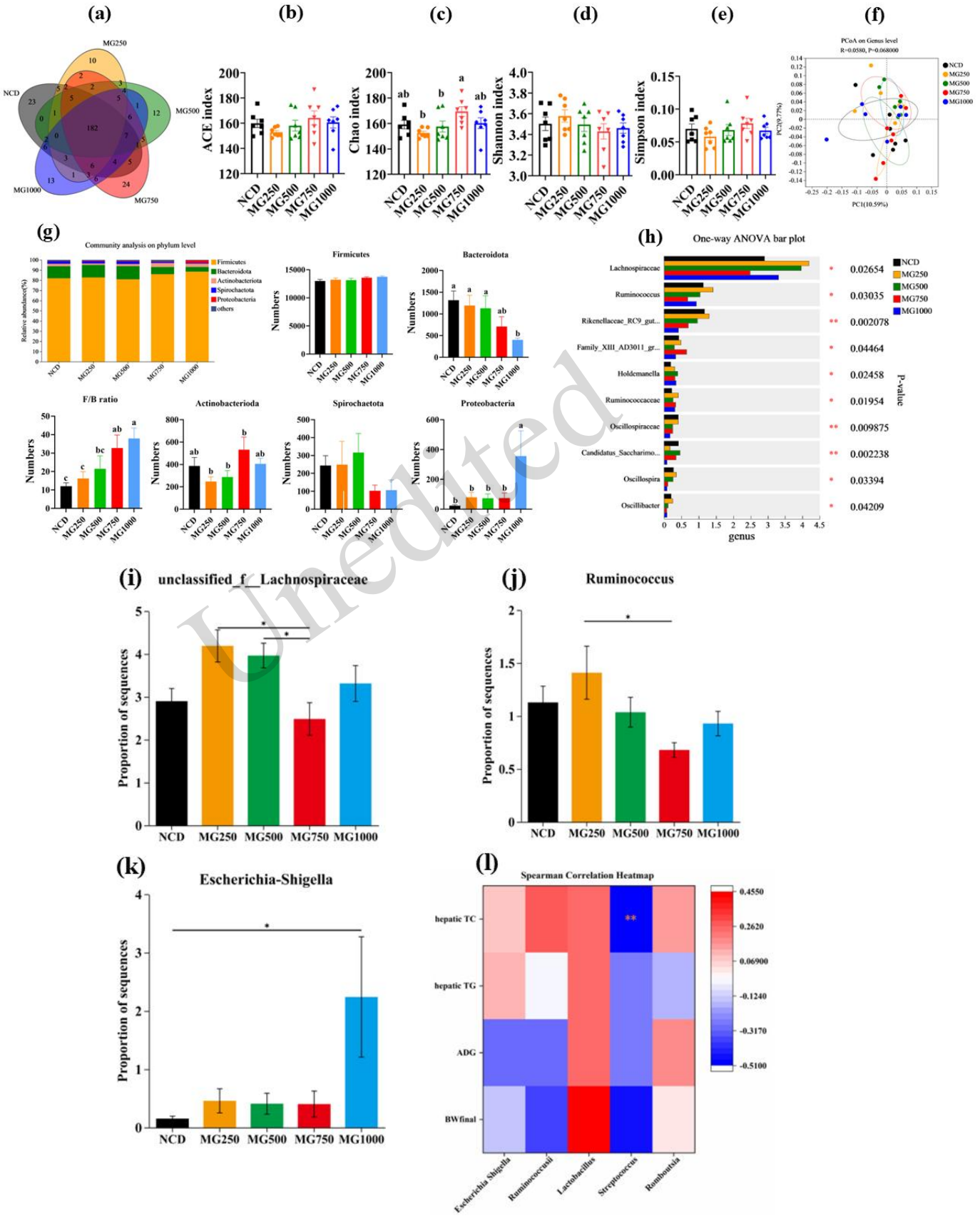
(a)
(b)
(c)
(d)
(e)
(f)
MG250
NCD
MG500
MG1000
MG750
ACE index
Chao index
Shannon index
Simpson index
PCoA on Genus level
R=0.0580, P=0.068000
PC1(10.59%)
PC2(9.77%)
(g)
Community analysis on phylum level
Relative abundance(%)
Firmicutes
Bacteroidota
Actinobacteriota
Spirochaetota
Proteobacteria
others
Numbers
F/B ratio
Actinobacterioda
Spirochaetota
Proteobacteria
(h)
One-way ANOVA bar plot
Lachnospiraceae
Ruminococcus
Rikenellaceae_RC9_gut...
Family_XIII_AD3011_gr...
Holdemanella
Ruminococcaceae
Oscillospiraceae
Candidatus_Saccharimo...
Oscillospira
Oscillibacter
P-value
genus
(i)
unclassified_f__Lachnospiraceae
Proportion of sequences
(j)
Ruminococcus
(k)
Escherichia-Shigella
(l)
Spearman Correlation Heatmap
hepatic TC
hepatic TG
ADG
BW final
Escherichia Shigella
Ruminococcus1
Lactobacillus
Streptococcus
Romboutsia

Figure 7 Effect of different doses of MG on gut microbiota. (a) Venn diagram; (b) ACE index; (c) Chao index; (d) Shannon index; (e) Simpson index; (f) Principal coordinate analysis (PCoA) chart; (g) gut microbiota composition at the phylum level. F/B ratio: Firmicutes / Bacteroidetes ratio. (h) Gut microbiota composition at the genus level; (i) relative abundance of *Lachnospiraceae*; (j) relative abundance of *Ruminococcus*; (k) relative abundance of *Escherichia/Shigella*; (l) Spearman correlation analysis. Different letters indicates significant difference ($p < 0.05$). * indicates $p < 0.05$, ** indicates $p < 0.01$. The values are expressed as mean ± standard error of the mean (SEM), n=7. TG: total triglyceride, TC: total cholesterol, BW_{final}: final weight, ADG: average daily weight gain.

4 Discussion

The growth rate and health status of pigs are directly related to market competitiveness and breeding efficiency. Compared with foreign pig breeds, although Chinese native pigs have unique advantages in terms of meat quality, their slow growth rate and high breeding costs are key restrictive factors of their market performance. The optimization of feed formula is a quick and simple solution to this challenge. To this end, many studies have confirmed that MG effectively improves the growth performance and health status of farmed animals, such as broiler chickens and yellow croakers (Luo et al., 2022). MG are allowed to be used as feed additives in China; however, the effect of MG on finishing pigs is still unclear. In the past few years, MG have been widely studied in weaned piglets and sows to improve weaning diarrhea, systemic inflammation, reproductive performance, and nutritional digestion (Park et al., 2024, Li et al., 2025, Li et al., 2022). In this study, we investigated the effects of MG supplementation on the growth and health of finishing pigs. The results showed that MG significantly promoted the production performance of finishing pigs, described as increased BW_{final}, ADG, SR, and decreased FCR and BT. MG intervention did not significantly affect glucolipid metabolism, the biomarkers of liver and kidney function, and the level of appetite hormone in the serum, suggesting that the growth promotion effect of MG was not derived from obesity or increased appetite. On the contrary, MG not only failed to cause obesity but also significantly improved visceral fat accumulation and systemic inflammation in mice fed with a high-fat diet (Zhang et al., 2023). Compared with lauric acid and lauric acid triglycerides, GML had a better regulatory effect on visceral fat deposition and glucose tolerance (Zhao et al., 2022). These results suggested that MG alleviated visceral fat deposition, which contributed to the liver health of finishing pigs. The 750 mg/kg dose of MG significantly reduced lipid deposition and cellular vacuolization in the liver, and the TG and TC contents were also reduced, but this dose had no significant effect on hepatic fatty acids composition, indicating that MG promoted weight gain by regulating the body's health status. A similar conclusion could also be obtained from other farmed animals. For example, GML improved the weight gain and reduced the FCR of whiteleg shrimp (*Penaeus vannamei*) by promoting lipid metabolism and reducing lipid accumulation (Liu et al., 2024). In a few words, at the appropriate dose, MG supplementation effectively promoted growth performance and improved hepatic health in Dongliao black finishing pigs.

Bile acids constitute an important physiological factor in lipid and nutrient absorption, along with signaling molecules that regulate glucolipid metabolism and energy balance, participating in bidirectional communication between host metabolism and gut microbiota (Chiang, 2013). Bile acids are synthesized from cholesterol in the liver and secreted into the small intestine to promote the emulsification and absorption of lipophilic substances. About 95% of bile acids are reabsorbed into the liver through the enterohepatic circulation, and only a small portion is excreted out through the feces (Dawson, Lan, & Rao, 2009). In this study, we confirmed that commercial diet-fed Dongliao black pigs exhibited massive lipid deposition in the liver, which might be ascribed to the fact that Dongliao black pigs possess certain susceptibility genes associated with obesity (Huang et al., 2024). However, MG intervention significantly increased TBA content in the liver and feces, reduced hepatic lipid content, and increased fecal lipid content, suggesting that MG exerted a lipid-lowering effect by metabolizing hepatic lipids to synthesize bile acids. Mechanistically, 750 mg/kg of MG significantly increased

the gene expression of *HMGCR* in the liver, indicating that MG promoted cholesterol synthesis, which could provide raw materials and substrates for bile acid synthesis. Based on the metabolic pathways and production sites, bile acids can be divided into primary bile acids and secondary bile acids. Primary bile acids are generated in the liver through a series of enzymatic reactions involving two main metabolic pathways, namely the classical pathway and the alternative pathway (Fiorucci et al., 2024). After being excreted into the intestine, primary bile acids are transformed by intestinal bacteria into different forms of secondary bile acids. The key enzymes of the classical pathway are *CYP7A1*, *CYP8B1* and *CYP27A1*, while the key enzymes of the alternative pathway are *CYP27A1* and *CYP7B1*. The classical pathway mainly produces cholic acid and chenodeoxycholic acid, which account for 90% of TBA in the physiological environment, and the alternative pathway mainly generates chenodeoxycholic acid (Fiorucci et al., 2021). This study found that 750 mg/kg of MG significantly increased the gene expression of *CYP7A1* but had no significant effect on the gene expression of *CYP27A1*, *CYP8B1* and *CYP7B1*, indicating that MG mainly converts cholesterol to bile acids through classical pathways, thereby reducing lipid accumulation in the liver. Similarly, quercetin alleviates hepatic lipid accumulation induced by type 2 diabetes through the *CYP7A1*-mediated conversion of cholesterol to bile acid (Yang et al., 2023).

After being synthesized in the liver, bile acids usually need to bind with glycine or taurine to form conjugated bile acids. In addition, bile acids can also be enzymatically modified through *UGT* or *SULT* to form other conjugated bile acids, thereby accelerating the efflux of bile acids by enhancing their water solubility and reducing their reabsorption capacity (Fiorucci et al., 2024). Our results demonstrated that MG at 750 mg/kg significantly increased the gene expression of *UGT2B4*, indicating that this promotive effect was achieved by enhancing the glucuronidation modification of bile acids. *SLC10A1* is a key bile salt transporter protein that maintains enterohepatic circulation, mainly expressed on the basolateral membrane of liver cells. It is the main active transport pathway for bile salts from the blood to the liver (Goutam et al., 2022). After MG intervention, the gene expression of *SLC10A1* in the liver was significantly upregulated, which facilitated the transport of bile acids from the blood to the liver, thereby accelerating enterohepatic circulation. Therefore, this study confirmed that MG intervention accelerated the conversion of cholesterol to bile acids, promoted bile acid excretion by enhancing glucuronidation modification and enterohepatic circulation, and finally alleviated liver fat deposition. However, based on the present results, the signaling pathway mediated by MG was not identified because there were no significant differences in gene expression related to peroxisome proliferator-activated receptors (PPAR) and AMP-activated protein kinase (AMPK) pathways, which therefore needed to be further investigated. In summary, it was revealed for the first time that MG reduces hepatic lipid deposition in black pigs through bile acid metabolism. Mechanistically, MG promotes the conversion of hepatic lipids into bile acids and facilitates their excretion by enhancing the water-soluble modification of bile acids. In addition, MG increases the content of fecal lipids, which might be due to MG inhibiting the absorption of dietary lipids and promoting their metabolism.

Gut microbiota colonized in the gastrointestinal tract of farmed animals interact with feed and hosts to maintain gastrointestinal homeostasis and host health (Kong et al., 2022). As a common food emulsifier and preservative, MG has a strong antibacterial property. In addition, previous studies have also elucidated the different regulatory effects of MG on gut microbiota. For example, GML selectively increased the relative abundance of *Bifidobacterium pseudolongum* in the gut to improve inflammation and lipid metabolism, and this beneficial effect was eliminated after antibiotic treatment, indicating that gut microbiota has a key role in the anti-obesity activity of GML (Zhao et al., 2020). In addition, the beneficial effects of GML could also be reflected in intergenerational inheritance: maternal supplementation with GML enhanced the intestinal barrier function of suckling piglets and reduced the relative abundance of *Escherichia/Shigella* (Zhao et al., 2023). In this study, we found that MG had no significant effect on the abundance and diversity of rectal microbiota compared with the NCD group. Although MG at 250 mg/kg and 750 mg/kg had similar growth-promoting effects, liver health in the two groups was quite different, which might be attributed to the fact that the relative abundances of *Lachnospiraceae* and *Ruminococcus* in the MG250 group were significantly higher than those in

the MG750 group, because the two bacteria are closely linked to obesity and diabetes (Sun et al., 2020; Xu et al., 2022). Furthermore, in our previous study, 150 mg kg^{-1} of GML induced metabolic syndrome by significantly increasing weight gain, fat droplet size, percentage of epididymal fat, liver weight, and systemic low-grade inflammation in low-fat diet fed mice (Jiang et al., 2018). Similarly, we found that MG at 250 mg/kg induced significant weight gain, with thickened backfat and hepatic fat deposition. Therefore, the results induced by 250 mg/kg of MG might be due to the combined effect of gut microbiota and hepatic lipid metabolism disorders. Moreover, compared with the other four groups, 1000 mg/kg of MG significantly increased the relative abundance of *Escherichia/Shigella*. The altered abundance of this bacterium might be one of the reasons for its poor effect, because the enrichment of *Escherichia/Shigella* has been related to intestinal diseases and diabetes (Jia et al., 2022). Besides, the enrichment of *Escherichia/Shigella* was negatively correlated with weight gain and ADG, and it was positively correlated with hepatic TC and TG, consistent with the trends of growth performance and hepatic fat deposition.

5 Conclusions

This study investigated the effects of MG on the growth and health of Dongliao black finishing pigs. The results showed that MG supplementation significantly improved the production performance of pigs without causing any metabolic syndrome or liver and kidney damage. MG at the dose of 750 mg/kg of significantly alleviated liver fat deposition via promoting the de novo synthesis of cholesterol, the conversion of cholesterol to bile acids, and enhancing bile acid modification and intestinal excretion. Furthermore, MG had no significant effect on the gut microbiota of the rectum. In summary, MG could be used as a feed additive with hepatoprotective and detoxifying effects to improve the growth and liver health of finishing pigs, and the optimal dietary MG requirement was determined to be 750 mg/kg.

Data availability statement

The data that support the findings of this study are available on request from the corresponding author. The data are not publicly available due to privacy or ethical restrictions.

Acknowledgments

This work was supported by the National Key Research and Development Program of China (No. 2023YFD2201300) and the National Natural Science Foundation of China (No 32372316 and 321722141) and the Qizhen Innovation Concept Program of Zhejiang University (No. GNYZ-XMRW-202301).

Authorship contribution

Nanhai Xiao: Conceptualization, Methodology, Formal analysis, Writing – original draft, Software, Review and editing. Xutang Wang: Investigation and Data analysis. Jing Wang: Investigation, Supervision. Fengqin Feng and Minjie Zhao: Supervision, Project administration, Fund acquisition, Writing and review.

Compliance with ethics guidelines

Nanhai XIAO, Xutang WANG, Jing WANG, Fengqin FENG, Minjie ZHAO declare that they have no known competing financial interests or personal relationships. All experimental procedures were approved by the Institutional Animal Ethics Committee of Zhejiang University (ZJU20240866). Every effort was made during the experiments to minimize animal suffering. All the institutional and national guidelines for the care and use of animals were followed.

References

Chiang JY, 2013. Bile acid metabolism and signaling. *Compr physiol*, 3(3): 1191-1212.

Dawson PA, Lan T, Rao A, 2009. Bile acid transporters. *J Lipid Res*, 50(12): 2340-2357.

Fiorucci S, Distrutti E, Carino A, et al., 2021. Bile acids and their receptors in metabolic disorders. *Prog Lipid Res*, 82: 101094.

Fiorucci S, Marchianò S, Urbani G, et al., 2024. Immunology of bile acids regulated receptors. *Prog Lipid Res*, 101291.

Gao Y, Li ZH, Zhang Q, et al., 2024. Comparison of meat quality, muscle-fibre characteristics and the Sirt1/AMPK/PGC-1α pathway in different breeds of pigs. *Anim Prod Sci*, 64(10).

Goutam K, Ielasi FS, Pardon E, et al., 2022. Structural basis of sodium-dependent bile salt uptake into the liver. *Nature*, 606(7916): 1015-1020.

Huang M, Zhang WY, Dong JP, et al., 2025. Genome-wide association studies of body weight and average daily gain in Chinese Dongliao black pigs. *Int J Mol Sci*, 26(7): 3453.

Jia M, Li DD, Wang R, et al., 2022. Gut microbiota derived structural changes of phenolic compounds from colored rice and its corresponding fermentation property. *Food Funct*, 13(20): 10759-10768.

Jiang ZL, Zhao MJ, Zhang H, et al., 2018. Antimicrobial emulsifier–glycerol monolaurate induces metabolic syndrome, gut microbiota dysbiosis, and systemic low-grade inflammation in low-fat diet fed mice. *Mol Nutr Food Res*, 62(3): 1700547.

Kong LL, Wang ZH, Xiao CP, et al., 2022. Glycerol monolaurate attenuated immunological stress and intestinal mucosal injury by regulating the gut microbiota and activating AMPK/Nrf2 signaling pathway in lipopolysaccharide-challenged broilers. *Anim Nutr*, 10: 347-359.

Li D, Yang M, Ma Z, et al., 2025. Glycerol monolaurate complex improved antioxidant, anti-Inflammation, and gut microbiota composition of offspring in a sow–piglet model. *Vet Sci*, 12(1): 24.

Li LX, Wang HK, Zhang N, et al., 2022. Effects of α-glycerol monolaurate on intestinal morphology, nutrient digestibility, serum profiles, and gut microbiota in weaned piglets. *J Anim Sci*, 100(3): skac046.

Liu RZ, Ding YJ, Jing FT, et al., 2024. Effects of dietary glycerol monolaurate on growth and digestive performance, lipid metabolism, immune defense and gut microbiota of shrimp (*Penaeus vannamei*). *Fish Shellfish Immun*, 151: 109666.

Liu T, Li C, Zhong H, et al., 2021. Dietary medium-chain α-monoglycerides increase BW, feed intake, and carcass yield in broilers with muscle composition alteration. *Poultry Sci*, 100(1): 186-195.

Liu T, Mo QF, Zhao MJ, et al., 2021. Mass spectrometry-based metabolomics to reveal chicken meat improvements by medium-chain monoglycerides supplementation: Taste, fresh meat quality, and composition. *Food Chem*, 365: 130303.

Liu T, Ruan SY, Mo QF, et al., 2023. Integrated serum metabolome and gut microbiome to decipher chicken amino acid improvements induced by medium-chain monoglycerides. *Metabolites*, 13(2): 208.

Liu WX, Luo XL, Huang Y, et al., 2023. Butyric-lauric acid structural lipid relieves liver inflammation and small intestinal microbial disturbance: In obese male C57BL/6 mice. *Food Biosci*, 55: 102944.

Luo XL, Liu WX, Zhao MJ, et al., 2022. Glycerol monolaurate beyond an emulsifier: Synthesis, in vivo fate, food quality benefits and health efficacies. *Trends Food Sci Tech*, 127: 291-302.

Park S, Sun S, Kovanda L, et al., 2024. Effects of monoglyceride blend on systemic and intestinal immune responses, and gut health of weaned pigs experimentally infected with a pathogenic Escherichia coli. *J Anim Sci Biotech*, 15(1): 141.

Silveira RF, Roque-Borda CA, Vicente EF, 2021. Antimicrobial peptides as a feed additive alternative to animal production, food safety and public health implications: An overview. *Anim Nutr*, 7(3): 896-904.

Sun XW, Zhao HL, Liu ZL, et al., 2020. Modulation of gut microbiota by fucoxanthin during alleviation of obesity in high-fat diet-fed mice. *J Agri Food Chem*, 68(18): 5118-5128.

Tu T, Wu WD, Tang XY, et al., 2021. Screening out important substances for distinguishing Chinese indigenous pork and hybrid pork and identifying different pork muscles by analyzing the fatty acid and nucleotide contents. *Food Chem*, 350: 129219.

Xu ZL, Jiang W, Huang WL, et al., 2022. Gut microbiota in patients with obesity and metabolic disorders—A

systematic review. *Genes Nutr*, 17(1): 2.

Yang MY, Zhang JH, Yan H, et al., 2024. A comprehensive review of medium chain monoglycerides on metabolic pathways, nutritional and functional properties, nanotechnology formulations and applications in food system. *Crit Revs Food Sci*, 65(15): 1-22.

Yang TT, Wang YY, Cao XY, et al., 2023. Targeting mTOR/YY1 signaling pathway by quercetin through CYP7A1-mediated cholesterol-to-bile acids conversion alleviated type 2 diabetes mellitus induced hepatic lipid accumulation. *Phytomedicin*e, 113: 154703.

Zhang JH, Liu T, Tang J, et al., 2023. Food additive glycerol monocaprylate modulated systemic inflammation and gut microbiota without stimulating metabolic dysfunction in high-fat diet fed mice. *Food Res Int*, 167: 112734.

Zhao H, Tian M, Xiong L, et al., 2023. Maternal supplementation with glycerol monolaurate improves the intestinal health of suckling piglets by inhibiting the NF-κB/MAPK pathways and improving oxidative stability. *Food Funct*, 14(7): 3290-3303.

Zhao MJ, Jiang ZL, Cai HY, et al., 2020. Modulation of the gut microbiota during high-dose glycerol monolaurate-mediated amelioration of obesity in mice fed a high-fat diet. *MBio*, 11(2).

Zhao MJ, Zhang JH, Liu T, et al., 2022. Differential modulations of lauric acid and its glycerides on high fat diet-induced metabolic disorders and gut microbiota dysbiosis. *Food Res Int*, 157: 111437.

Supplementary information:

Table S1 The composition and nutrient levels of basal diets (%DM)

Ingredients	Levels (%)	Nutrient levels[2]	levels
Corn	9.5	Digestible energy (kcal/kg)	2875.0
Wheat	10	Crude protein (%)	13
Brown rice	10	Crude fiber (%)	10
Barley	15	Crude ash (%)	8
Flour	8.5	Calcium (%)	0.8
Barley roots	12	Phosphorus (%)	0.25
Alfalfa	9	Sodium chloride (%)	0.6
Yellow wine lees	8	Copper (ppm)	25
Rice bran meal	8	Lysine (%)	0.95
Corn germ meal	6	OM	96.0%
Premix feed[1]	4		
Total	100		

[1] Premix feed provided the following per kg of the diet: $CuCl_2$ 10 mg, $FeSO_4$ 70 mg, $ZnSO_4$ 20 mg, $MnSO_4$ 10 mg, $Ca(IO_3)_2$ 1 mg, Na_2SeO_3 0.3 mg, $CoSO_4$ 0.6 mg, vitamin A 3000 IU, vitamin D_3 1050 IU, vitamin E 200 mg, vitamin K_3 10.4 mg, vitamin B_1 8.5 mg, vitamin B_2 21.1 mg, vitamin B_6 11.7 mg, vitamin B_{12} 0.1 mg, vitamin H 0.52 mg, folic acid 3.2 mg, nicotinamide 101 mg, D- pantothenic acid 55.2 mg, choline chloride 300 mg.
[2] Values of digestible energy were calculated. Crude protein and other nutrient levels were measured values.
DM = dry matter, OM = organic matter.

Table 2 The primer sequences

Gene	Forward primer	Reverse primer
GAPDH	TCGGAGTGAACGGATTTGGC	TGACAAGCTTCCCGTTCTCC
HMGCR	AAGCGAGTGGTCCCACAAAT	CTTTGCACGCTCCTTGAACC
DHCR7	GTACCTGGTTTACCACCCCG	GCCGAAACAGGTCCTTCTGA
CYP7A1	GAGTTCCTCCGAGCAAACCA	CCATCACTGGGGTCAATGCT
CYP27A1	TTGAGAAACGCATTGGCTGC	ATCCAGGTATCGCCTCCAGT

CYP7B1	CCCTGTTGCTGCTGGTCTTATT	CTTCTCCAATGAAAGGAAGCCA
CYP8B1	TGGTGGCCATTGTGGGATAC	CGGTGAATATGTCCCCGTGT
UGT2B4	GAAGAACTCCAAGTTCGCGG	GAAGTTGGAGGATCTCCGCAT
UGT2C1	CGTCAAGTTCACACGAATGCT	GCCTGCTGAGTAACTCCTTGT
SLC10A1	ACGTTCAACTCTGCTCCACC	ATCAGCTGCGGAGATCGTTT
SREBP1c	GCGAGTCAAGACCAGTCTCC	TCCCCATCCACGAAGAAACG
FAS	CGTTGGGTCGACTCACTGAA	GAGACAGTTCACCATGCCCA
ACC	CCAGCACTCCCGCTTCATAA	GTAAGGCCAAGCCATCCTGT
SCD-1	GCCACCTTTCTTCGTTACGC	CCTCACCCACAGCTCCCAAT
CPT-1	CAAGATAGCGGCCGAAAAGC	GATAATCGCCACGGCTCAGA

GAPDH: glyceraldehyde-3-phosphate dehydrogenase, *HMGCR*: HMG-CoA reductase, *DHCR7*: 7-dehydrocholesterol reductase, *CYP*: cytochrome P450, *UGT*: UDP-glucuronyl transferase, *SLC10A1*: solute carrier family 10 member 1, *FAS*: fatty acid synthetase, *SREBP-1c*: sterol regulatory element binding proteins-1c, *ACC*: Acetyl-CoA carboxylase, *SCD-1*: Stearoyl-CoA Desaturase 1, *CPT-1*: carnitine palmitoyltransferase 1.

Table 3 The sequencing result of transcriptome

Sample	Raw reads	Raw bases	Clean reads	Clean bases	Error rate (%)	Q20(%)	Q30(%)	GC content (%)
NCD1	44576908	6731113108	44228286	6636873814	0.0118	98.82	96.34	50.96
NCD2	42508296	6418752696	42158902	6308779057	0.0118	98.82	96.34	50.77
NCD3	40989988	6189488188	40687906	6096053698	0.0118	98.85	96.4	50.49
NCD4	43851110	6621517610	43518676	6523363081	0.0118	98.81	96.31	50.76
NCD5	44196580	6673683580	43870408	6593672876	0.0118	98.85	96.42	50.69
MG750_1	43603110	6584069610	43279676	6491525081	0.0118	98.84	96.4	50.85
MG750_2	58929516	8898356916	58441940	8770511571	0.0121	98.63	95.91	51.23
MG750_3	50722288	7659065488	50336568	7545958030	0.0121	98.63	95.82	51.43
MG750_4	49100784	7414218384	48698130	7315576353	0.0121	98.61	95.83	51.12
MG750_5	47203010	7127654510	46791642	7019083814	0.0121	98.62	95.86	49.62

Table 4 The alignment rate of clean data

Sample	Total reads	Total mapped	Multiple mapped	Uniquely mapped
NCD1	44228286	42810380(96.79%)	1619528(3.66%)	41190852(93.13%)
NCD2	42158902	40782636(96.74%)	1666869(3.95%)	39115767(92.78%)
NCD3	40687906	39467609(97.0%)	1540818(3.79%)	37926791(93.21%)
NCD4	43518676	42191464(96.95%)	1702123(3.91%)	40489341(93.04%)
NCD5	43870408	42617206(97.14%)	1698880(3.87%)	40918326(93.27%)
MG750_1	43279676	41947648(96.92%)	1805433(4.17%)	40142215(92.75%)

MG750_2	58441940	56439388(96.57%)	2544760(4.35%)	53894628(92.22%)
MG750_3	50336568	48751484(96.85%)	2282328(4.53%)	46469156(92.32%)
MG750_4	48698130	47032570(96.58%)	1827084(3.75%)	45205486(92.83%)
MG750_5	46791642	45168460(96.53%)	1933962(4.13%)	43234498(92.4%)